Thermal Emission from a Layered Medium Bounded by a Slightly Rough Interface

Joel T. Johnson, *Member, IEEE*

***Abstract*—The small perturbation method (SPM) is applied to study thermal emission from a layered medium bounded by a slightly rough interface. Brightness temperatures are calculated to second order in surface height, including both specular reflection coefficient corrections and incoherent Bragg scatter terms. Unlike the homogeneous medium case, in which the SPM applied for emission predictions produces an expansion in surface slope, the theory remains a small height expansion, and convergence of the series is shown to depend on properties of the layered medium. Results from this theory can be applied in studies of soil moisture, sea ice, or sea surface remote sensing and buried object detection with microwave radiometers.**

***Index Terms*—Microwave radiometry, remote sensing, rough surfaces.**

I. Introduction

MODELS for microwave thermal emission from deterministic or statistically described rough surfaces are of interest in passive remote sensing of soil moisture, sea ice, and the ocean surface. Several models for thermal emission from a rough surface bounding a homogeneous medium have been developed previously [1]–[6], primarily through application of standard surface scattering approximate methods to calculate surface emissivity using Kirchhoff's law. Models based on both the small perturbation method (SPM) and the physical optics (PO) approximation have been presented. A recent work [7] has further revealed that use of the SPM for emission from a rough surface bounding a homogeneous medium results in a small slope (rather than small height) emission approximation identical to that which would be obtained from the small slope approximation of [8]. The SPM can thus provide accurate emission predictions even for surfaces with large heights in terms of the electromagnetic wavelength. Numerical tests of the SPM for a set of canonical periodic surfaces have confirmed this statement [9]. These results motivate use of the SPM/small slope approximation (SPM/SSA) for the study of homogeneous medium thermal emission. However, the SPM for emission from a rough surface bounding a layered medium has apparently not previously been considered. This problem is potentially more relevant to soil moisture remote sensing studies given the variations in soil moisture content with depth which typically occur. A model for emission from a layered medium bounded by a rough interface could also be applied to model sea water covered with foam, ice, or other materials, or used to estimate surface clutter influences on microwave radiometry systems for buried object detection [10], [11].

The SPM has previously been applied to study backscattering from a layered medium bounded by a slightly rough interface [12]–[16] and results demonstrated that the presence of a layered medium can cause significant changes in first order surface scattered fields. An approximation for modifying two layer medium surface scattering predictions to the case of a finite object buried beneath a rough interface was also suggested in [12] for application to ground penetrating radar problems.

In this paper, the results of [12], [13] are extended to enable calculation of thermal emission from a slightly rough interface bounding a layered medium. Note that studies of thermal emission require both the first order SPM terms as in [12], [13] and also second order corrections to the specular reflection coefficient [2]. These quantities are derived and presented in Sections II and III. As in the homogeneous medium case, the resulting expression for the rough surface-induced correction to flat surface brightness temperatures is expressed in terms of an integral over the surface directional spectrum multiplied by a "weighting" function [17]. Studies of the weighting functions allow properties of the emission physics to be inferred independent of the surface statistics considered. Consideration of the weighting functions for isotropic (i.e., azimuthally symmetric) surfaces in Section IV reveals that a small height and not small slope expansion is obtained in the layered medium case, and convergence properties of this series are discussed. Studies of the weighting functions for azimuthally asymmetric surfaces in Section V again show a small height expansion for the second and higher azimuthal harmonics of all polarimetric brightness temperatures. Sample results applying the theory are presented in Section VI, and implications of the study considered in Section VII.

II. Formulation

A systematic solution of SPM equations for scattering from a rough surface bounding a homogeneous medium has recently been developed in [18]. This procedure applies the Rayleigh hypothesis to study scattered and transmitted plane wave amplitudes from a periodic surface excited by an incident plane wave, as in the original SPM formulation of [19]. SPM results for a nonperiodic surface are obtained in the limit as the surface periods become large following [19], [20]. The same procedure is applied in this paper for a rough surface bounding a layered

Manuscript received July 23, 1999; revised June 15, 2000. This work was sponsored by the Office of Naval Research, Washington, DC, Contract N00014-97-1-0541, National Science Foundation, Washington, DC, Project ECS-9701678, and by a Grant from Duke University, Durham, NC, as part of the OSD MURI on Humanitarian Demining.

The author is with the Department of Electrical Engineering and Electro-Science Laboratory, The Ohio State University, Columbus, OH 43210.

Publisher Item Identifier S 0196-2892(01)01157-3.

medium. The details of the procedure are very similar to [18], so only the basic formulation and results from the method are summarized here.

Consider a zero mean periodic surface profile $z = f(x, y)$ with periods P_x and P_y in the x and y directions, respectively, which separates free space in region zero (permittivity ϵ_0, permeability μ_0) for $z > f(x, y)$ from region one, a homogeneous nonmagnetic dielectric medium with permittivity $\epsilon_d = \epsilon\epsilon_0$ for $-d < z < f(x, y)$. Initially, a two layer configuration is considered, with Region 2 for $z < -d$ a homogeneous nonmagnetic dielectric medium with permittivity $\epsilon_{d2} = \epsilon_2\epsilon_0$ as illustrated in Fig. 1. Extension to a multilayer medium is straightforward and will be described below. The periodic surface $f(x, y)$ can also be expressed in terms of its Fourier series coefficients

$$f(x, y) = \sum_{n=-\infty}^{\infty} \sum_{m=-\infty}^{\infty} \exp\left(i\frac{2\pi nx}{P_x}\right)\exp\left(i\frac{2\pi my}{P_y}\right) h_{n,m} \tag{1}$$

$$h_{n,m} = \frac{1}{P_x}\frac{1}{P_y}\int_0^{P_x} dx \int_0^{P_y} dy \exp\left(-i\frac{2\pi nx}{P_x}\right) \cdot \exp\left(-i\frac{2\pi my}{P_y}\right) f(x, y). \tag{2}$$

Consider an incident electromagnetic plane wave that illuminates this periodic surface from the free space region, with electric and magnetic fields given by

$$\overline{E}^i = \hat{e}_i \exp\left(i\overline{k}_i \cdot \overline{r}\right) \tag{3}$$

$$\overline{H}^i = \frac{\hat{k}_i \times \hat{e}_i}{\eta_0} \exp\left(i\overline{k}_i \cdot \overline{r}\right) \tag{4}$$

where $\hat{e}_i$ represents the polarization vector of the incident electric field.

$$\overline{k}_i = k_0\hat{k}_i = \hat{x}k_{xi} + \hat{y}k_{yi} - \hat{z}k_{zi} \tag{5}$$

represents the propagation vector of the incident plane wave with wavenumber $k_0 = 2\pi/\lambda$.

$$\overline{r} = \hat{x}x + \hat{y}y + \hat{z}z \tag{6}$$

is a position vector in Cartesian space, and $\eta_0 = \sqrt{(\mu_0/\epsilon_0)}$ is the impedance of free space. Note an $\exp(-i\omega t)$ time convention is assumed.

Under the Rayleigh hypothesis, the scattered field in region zero consists of a sum of upgoing plane waves (or "Floquet modes"), which can be written as

$$\overline{E}^s = \sum_m \sum_n \left[\hat{h}_s^{n,m}\alpha_{n,m} + \hat{v}_s^{n,m}\beta_{n,m}\right] \cdot \exp\left(i\overline{k}_s^{n,m} \cdot \overline{r}\right) \tag{7}$$

$$\overline{H}^s = \frac{1}{\eta_0}\sum_m \sum_n \left[-\hat{v}_s^{n,m}\alpha_{n,m} + \hat{h}_s^{n,m}\beta_{n,m}\right] \cdot \exp\left(i\overline{k}_s^{n,m} \cdot \overline{r}\right) \tag{8}$$

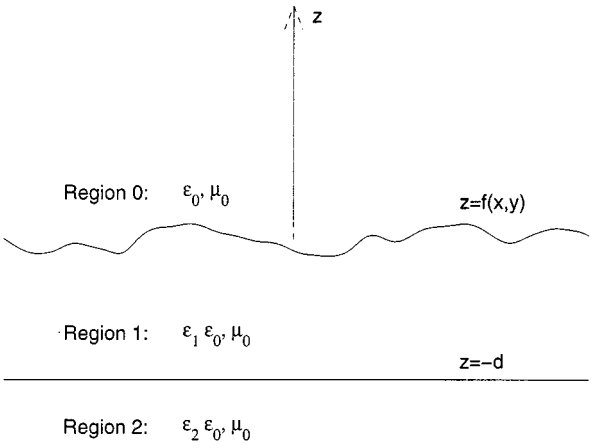

Fig. 1. Geometry of two layer medium bounded by a slightly rough interface.

while fields in region one consist of both upgoing and downgoing plane, waves which can be written as

$$\overline{E}^t = \sum_m \sum_n \left[\hat{h}_s^{n,m}\gamma_{n,m} + \hat{v}_t^{n,m}\delta_{n,m}\right] \cdot \exp\left(i\overline{k}_t^{n,m} \cdot \overline{r}\right) + \sum_m \sum_n \left[\hat{h}_s^{n,m}\Gamma_{n,m} + \hat{v}_u^{n,m}\Delta_{n,m}\right] \cdot \exp\left(i\overline{k}_u^{n,m} \cdot \overline{r}\right) \tag{9}$$

$$\overline{H}^t = \frac{1}{\eta_1}\sum_m \sum_n \left[-\hat{v}_t^{n,m}\gamma_{n,m} + \hat{h}_s^{n,m}\delta_{n,m}\right] \cdot \exp\left(i\overline{k}_t^{n,m} \cdot \overline{r}\right) + \frac{1}{\eta_1}\sum_m \sum_n \left[-\hat{v}_u^{n,m}\Gamma_{n,m} + \hat{h}_s^{n,m}\Delta_{n,m}\right] \cdot \exp\left(i\overline{k}_u^{n,m} \cdot \overline{r}\right) \tag{10}$$

where $\eta_1 = \eta_0/\sqrt{\epsilon}$ is the impedance of the lower medium. Note that all sums are assumed to be from $-\infty$ to ∞ unless otherwise notated. Fields in region two consist only of downgoing plane waves, written as

$$\overline{E}^l = \sum_m \sum_n \left[\hat{h}_s^{n,m}P_{n,m} + \hat{v}_l^{n,m}Q_{n,m}\right] \cdot \exp\left(i\overline{k}_l^{n,m} \cdot \overline{r}\right) \tag{11}$$

$$\overline{H}^l = \frac{1}{\eta_2}\sum_m \sum_n \left[-\hat{v}_l^{n,m}P_{n,m} + \hat{h}_s^{n,m}Q_{n,m}\right] \cdot \exp\left(i\overline{k}_l^{n,m} \cdot \overline{r}\right) \tag{12}$$

where $\eta_2 = \eta_0/\sqrt{\epsilon_2}$ is the impedance of the lower medium. In the above equation, α, β, γ, δ, Γ, Δ, P, and Q are the unknown complex amplitudes of the Floquet modes in each region. Plane wave propagation vectors are defined by the Floquet theorem as

$$\overline{k}_s^{n,m} = \hat{x}k_{xn} + \hat{y}k_{ym} + \hat{z}k_{znm} \tag{13}$$

$$\overline{k}_t^{n,m} = \hat{x}k_{xn} + \hat{y}k_{ym} - \hat{z}k_{z1nm} \tag{14}$$

$$\overline{k}_u^{n,m} = \hat{x}k_{xn} + \hat{y}k_{ym} + \hat{z}k_{z1nm} \tag{15}$$

$$\overline{k}_l^{n,m} = \hat{x}k_{xn} + \hat{y}k_{ym} - \hat{z}k_{z2nm} \tag{16}$$

where

$$k_{xn} = k_{xi} + \frac{2\pi n}{P_x} \tag{17}$$

$$k_{ym} = k_{yi} + \frac{2\pi m}{P_y} \tag{18}$$

$$k_{\rho nm} = \sqrt{k_{xn}^2 + k_{ym}^2} \tag{19}$$

$$k_{znm} = \sqrt{k_0^2 - k_{\rho nm}^2} \tag{20}$$

$$k_{z1nm} = \sqrt{k_0^2 \epsilon - k_{\rho nm}^2} \tag{21}$$

$$k_{z2nm} = \sqrt{k_0^2 \epsilon_2 - k_{\rho nm}^2}. \tag{22}$$

Modes for which $k_{\rho nm}$ becomes greater than k_0, k_1, or k_2 have k_{znm}, k_{z1nm}, and k_{z2nm}, respectively, defined so that attenuation occurs as upgoing fields propagate away from the rough surface in region zero and as downgoing fields propagate away from the layered medium boundaries in regions one and two. Orthogonal horizontal and vertical polarization vectors for these plane waves are defined as

$$\hat{h}_i = \hat{x}\frac{k_{yi}}{k_{\rho i}} - \hat{y}\frac{k_{xi}}{k_{\rho i}} \tag{23}$$

$$\hat{h}_s^{n,m} = \hat{x}\frac{k_{ym}}{k_{\rho nm}} - \hat{y}\frac{k_{xn}}{k_{\rho nm}} \tag{24}$$

$$\hat{v}_i = \hat{x}\frac{k_{xi}k_{zi}}{k_0 k_{\rho i}} + \hat{y}\frac{k_{yi}k_{zi}}{k_0 k_{\rho i}} + \hat{z}\frac{k_{\rho i}}{k_0} \tag{25}$$

$$\hat{v}_s^{n,m} = -\hat{x}\frac{k_{xn}k_{znm}}{k_0 k_{\rho nm}} - \hat{y}\frac{k_{ym}k_{znm}}{k_0 k_{\rho nm}} + \hat{z}\frac{k_{\rho nm}}{k_0} \tag{26}$$

$$\hat{v}_t^{n,m} = \hat{x}\frac{k_{xn}k_{z1nm}}{k_1 k_{\rho nm}} + \hat{y}\frac{k_{ym}k_{z1nm}}{k_1 k_{\rho nm}} + \hat{z}\frac{k_{\rho nm}}{k_1} \tag{27}$$

$$\hat{v}_u^{n,m} = -\hat{x}\frac{k_{xn}k_{z1nm}}{k_1 k_{\rho nm}} - \hat{y}\frac{k_{ym}k_{z1nm}}{k_1 k_{\rho nm}} + \hat{z}\frac{k_{\rho nm}}{k_1} \tag{28}$$

$$\hat{v}_l^{n,m} = \hat{x}\frac{k_{xn}k_{z2nm}}{k_2 k_{\rho nm}} + \hat{y}\frac{k_{ym}k_{z2nm}}{k_2 k_{\rho nm}} + \hat{z}\frac{k_{\rho nm}}{k_2} \tag{29}$$

where $k_1 = k_0\sqrt{\epsilon}$ and $k_2 = k_0\sqrt{\epsilon_2}$ are the wavenumbers in regions one and two, respectively.

Boundary conditions on the layered medium interfaces specify that tangential electric and magnetic fields must be continuous. At $z = f(x, y)$, this becomes

$$(\hat{z} - \overline{\partial f}) \times (\overline{E}^i + \overline{E}^s) = (\hat{z} - \overline{\partial f}) \times \overline{E}^t \tag{30}$$

$$(\hat{z} - \overline{\partial f}) \times (\overline{H}^i + \overline{H}^s) = (\hat{z} - \overline{\partial f}) \times \overline{H}^t \tag{31}$$

since a vector normal to the surface can be written as $\hat{z} - \overline{\partial f}$, where $\overline{\partial f} = \hat{x}(\partial f/\partial x) + \hat{y}(\partial f/\partial y)$. At $z = -d$, the boundary conditions specify

$$\hat{z} \times \overline{E}^t = \hat{z} \times \overline{E}^l \tag{32}$$

$$\hat{z} \times \overline{H}^t = \hat{z} \times \overline{H}^l. \tag{33}$$

Substituting the Rayleigh hypothesis fields from (9)–(12) into (32), (33), the following relationships can be derived:

$$P_{n,m} = \gamma_{n,m} \exp(i(k_{z1nm} - k_{z2nm})\, d) \cdot \left(\frac{2k_{z1nm}}{k_{z1nm} + k_{z2nm}}\right) \tag{34}$$

$$Q_{n,m} = \delta_{n,m} \exp(i(k_{z1nm} - k_{z2nm})\, d) \cdot \left(\frac{2k_{z1nm}\sqrt{\epsilon\epsilon_2}}{\epsilon_2 k_{z1nm} + \epsilon k_{z2nm}}\right) \tag{35}$$

$$\Gamma_{n,m} = \gamma_{n,m} \exp(2ik_{z1nm}d) \left(\frac{k_{z1nm} - k_{z2nm}}{k_{z1nm} + k_{z2nm}}\right) \tag{36}$$

$$= \gamma_{n,m} \exp(2ik_{z1nm}d) R_h(k_{z1nm}, k_{z2nm}) \tag{37}$$

$$\Delta_{n,m} = \delta_{n,m} \exp(2ik_{z1nm}d) \left(\frac{\epsilon_2 k_{z1nm} - \epsilon k_{z2nm}}{\epsilon_2 k_{z1nm} + \epsilon k_{z2nm}}\right) \tag{38}$$

$$= \delta_{n,m} \exp(2ik_{z1nm}d) R_v(\epsilon_2 k_{z1nm}, \epsilon k_{z2nm}) \tag{39}$$

which defines the lower layer reflection coefficients $R_h(k_{z1nm}, k_{z2nm})$ and $R_v(\epsilon_2 k_{z1nm}, \epsilon k_{z2nm})$, respectively. These definitions make the generalization to a layered medium below the rough interface clear. $R_h(k_{z1nm}, k_{z2nm})$ and $R_v(\epsilon_2 k_{z1nm}, \epsilon k_{z2nm})$ are simply replaced by the reflection coefficients of the layered medium below $z = -d$. Expressions for $P_{n,m}$ and $Q_{n,m}$ are no longer correct in this case, but since thermal emission can be computed from the reflectivity in the region zero (i.e., in terms of α and β only), it is still possible to compute brightness temperatures for the layered medium by modifying only these reflection coefficients.

Substituting the above relationships and the Rayleigh hypothesis fields from (7)–(10) into (30), (31), the following equations result if only x and y components are considered:

$$\begin{aligned}
&\sum_m \sum_n \exp\left(i\frac{2\pi n x}{P_x}\right) \exp\left(i\frac{2\pi m y}{P_y}\right) \\
&\quad \cdot \Big[(\hat{z} \times \hat{h}_s^{n,m})(\alpha_{n,m} \exp(ik_{znm}z) - \gamma_{n,m} \\
&\qquad \cdot (\exp(-ik_{z1nm}z) + R_h(k_{z1nm}, k_{z2nm}) \\
&\qquad\quad \cdot \exp(2ik_{z1nm}d) \exp(ik_{z1nm}z))) + (\hat{z} \times \hat{v}_s^{n,m}) \\
&\qquad \cdot \Big(\beta_{n,m} \exp(ik_{znm}z) + \frac{k_0 k_{z1nm}}{k_1 k_{znm}} \delta_{n,m} \\
&\qquad\quad \cdot (\exp(-ik_{z1nm}z) - R_v(\epsilon_2 k_{z1nm}, \epsilon k_{z2nm}) \\
&\qquad\quad \cdot \exp(2ik_{z1nm}d) \exp(ik_{z1nm}z))\Big)\Big] \\
&= -(\hat{z} \times \hat{e}_i) \exp(-ik_{zi}z) + (\overline{\partial f} \times \hat{e}_i) \exp(-ik_{zi}z) \\
&\quad + \sum_m \sum_n \exp\left(i\frac{2\pi n x}{P_x}\right) \exp\left(i\frac{2\pi m y}{P_y}\right) \\
&\quad \cdot \Big[(\overline{\partial f} \times \hat{v}_s^{n,m}) \Big(\beta_{n,m} \exp(ik_{znm}z) - \frac{k_0}{k_1} \\
&\qquad \cdot \delta_{n,m}(\exp(-ik_{z1nm}z) + R_v(\epsilon_2 k_{z1nm}, \epsilon k_{z2nm}) \\
&\qquad\quad \cdot \exp(2ik_{z1nm}d) \exp(ik_{z1nm}z))\Big)\Big]
\end{aligned} \tag{40}$$

$$\begin{aligned}
&\sum_m \sum_n \exp\left(i\frac{2\pi n x}{P_x}\right) \exp\left(i\frac{2\pi m y}{P_y}\right) \\
&\quad \cdot \Big[(-\hat{z} \times \hat{v}_s^{n,m}) \Big(\alpha_{n,m} \exp(ik_{znm}z) + \frac{k_{z1nm}}{k_{znm}} \\
&\qquad \cdot \gamma_{n,m}(\exp(-ik_{z1nm}z) - R_h(k_{z1nm}, k_{z2nm}) \\
&\qquad\quad \cdot \exp(2ik_{z1nm}d) \exp(ik_{z1nm}z))\Big) \\
&\qquad + (\hat{z} \times \hat{h}_s^{n,m}) \Big(\beta_{n,m} \exp(ik_{znm}z) - \frac{k_1}{k_0}
\end{aligned}$$

$$\cdot \delta_{n,m}(\exp(-ik_{z1nm}z) + R_v(\epsilon_2 k_{z1nm}, \epsilon k_{z2nm}) \cdot \exp(2ik_{z1nm}d)\exp(ik_{z1nm}z))\Big)\Big]$$
$$= -(\hat{z}\times\hat{k}_i\times\hat{e}_i)\exp(-ik_{zi}z) + \Big(\overline{\partial f}\times\hat{k}_i\times\hat{e}_i\Big)\cdot\exp(-ik_{zi}z) + \sum_m\sum_n \exp\Big(i\frac{2\pi nx}{P_x}\Big)\exp\Big(i\frac{2\pi my}{P_y}\Big)\cdot\Big[\Big(-\overline{\partial f}\times\hat{v}_s^{n,m}\Big)(\alpha_{n,m}\exp(ik_{znm}z) - \gamma_{n,m}(\exp(-ik_{z1nm}z) + R_h(k_{z1nm}, k_{z2nm}) \cdot \exp(2ik_{z1nm}d)\exp(ik_{z1nm}z)))\Big]. \quad (41)$$

Note that the above equations (which have two components each) provide four scalar equations for the four scalar unknown functions α, β, γ, and δ, with unknowns Γ, Δ, P, and Q determined from (34)–(39).

At this point, a small height expansion is used by expanding the exponentials in the above equations in power series

$$\exp(\pm ik_z z) = \sum_{q=0}^{\infty}\frac{(\pm ik_z z)^q}{q!} \quad (42)$$

and by substituting a perturbation series for the unknowns

$$\alpha_{n,m} = \alpha_{n,m}^{(0)} + \alpha_{n,m}^{(1)} + \cdots = \sum_{l=0}^{\infty}\alpha_{n,m}^{(l)} \quad (43)$$

with similar definitions for β, γ, and δ. Perturbation series terms are defined so that the lth term is of order f^l or equivalent combinations of f and its derivatives since $(\partial f/\partial x)$ and $(\partial f/\partial y)$ are assumed to be the same order as f.

III. Solution of SPM Equations

The systematic procedure for solving SPM equations described in [18] is applied to (40) and (41) once the perturbation series is substituted. Solutions at the zeroth order are found to consist only of the specular plane waves in each region (represented by $n = m = 0$), with fields in region zero given by

$$\alpha_{0,0}^{(0)} = \frac{k_{zi} - k_{z1i}Z_h(k_{z1i}, k_{z2i}, d)}{k_{zi} + k_{z1i}Z_h(k_{z1i}, k_{z2i}, d)} = R_{Hl} \quad (44)$$
$$\beta_{0,0}^{(0)} = 0 \quad (45)$$

for a horizontally polarized incident field (i.e., $\hat{e}_i = \hat{h}_i$), while

$$\alpha_{0,0}^{(0)} = 0 \quad (46)$$
$$\beta_{0,0}^{(0)} = \frac{\epsilon k_{zi} - k_{z1i}Z_v(\epsilon_2 k_{z1i}, \epsilon_1 k_{z2i}, d)}{\epsilon k_{zi} + k_{z1i}Z_v(\epsilon_2 k_{z1i}, \epsilon_1 k_{z2i}, d)} = R_{Vl} \quad (47)$$

for a vertically polarized incident field. The above equations are the total reflection coefficients at $z = 0$ of the layered medium with a flat surface R_{Hl} and R_{Vl} and also involve

$$Z_h(k_{z1nm}, k_{z2nm}, d) = \frac{1 - R_h(k_{z1nm}, k_{z2nm})\exp(2ik_{z1nm}d)}{1 + R_h(k_{z1nm}, k_{z2nm})\exp(2ik_{z1nm}d)} = \frac{1 - G_h(k_{z1nm}, k_{z2nm}, d)}{1 + G_h(k_{z1nm}, k_{z2nm}, d)}$$
$$Z_v(\epsilon_2 k_{z1nm}, \epsilon k_{z2nm}, d) = \frac{1 - R_v(\epsilon_2 k_{z1nm}, \epsilon k_{z2nm})\exp(2ik_{z1nm}d)}{1 + R_v(\epsilon_2 k_{z1nm}, \epsilon k_{z2nm})\exp(2ik_{z1nm}d)} = \frac{1 - G_v(\epsilon_2 k_{z1nm}, \epsilon k_{z2nm}, d)}{1 + G_v(\epsilon_2 k_{z1nm}, \epsilon k_{z2nm}, d)}. \quad (48)$$

A general form for first order solutions is

$$\zeta_{n,m}^{(1)} = h_{n,m}g_\zeta^{(1)}(k_{xn}, k_{ym}) \quad (49)$$

where $\zeta = \alpha$, β, γ, or δ, and $g_\zeta^{(1)}$ is a corresponding function. Solutions in region zero for a horizontally polarized incident field are

$$g_\alpha^{(1)} = \frac{-2ik_{zi}(k_0^2 - k_1^2)}{(k_{znm} + k_{z1nm})(k_{zi} + k_{z1i})}c_{i,n} \cdot\left[\frac{1 + G_h(k_{z1i}, k_{z2i}, d)}{1 + G_h(k_{z1i}, k_{z2i}, d)R_h(k_{zi}, k_{z1i})}\right]\left[\frac{1 + G_h(k_{z1nm}, k_{z2nm}, d)}{1 + G_h(k_{z1nm}, k_{z2nm}, d)R_h(k_{znm}, k_{z1nm})}\right] \quad (50)$$

$$g_\beta^{(1)} = \frac{-2ik_{zi}(k_0^2 - k_1^2)}{(\epsilon k_{znm} + k_{z1nm})(k_{zi} + k_{z1i})}\left(\frac{k_{z1nm}}{k_0}\right)s_{i,n} \cdot\left[\frac{1 + G_h(k_{z1i}, k_{z2i}, d)}{1 + G_h(k_{z1i}, k_{z2i}, d)R_h(k_{zi}, k_{z1i})}\right] \cdot\left[\frac{1 - G_v(\epsilon_2 k_{z1nm}, \epsilon k_{z2nm}, d)}{1 + G_v(\epsilon_2 k_{z1nm}, \epsilon k_{z2nm}, d)R_v(\epsilon k_{znm}, k_{z1nm})}\right] \quad (51)$$

while

$$g_\alpha^{(1)} = \frac{-2ik_{zi}(k_0^2 - k_1^2)}{(k_{znm} + k_{z1nm})(\epsilon k_{zi} + k_{z1i})}\left(\frac{k_{z1i}}{k_0}\right)s_{i,n} \cdot\left[\frac{1 + G_h(k_{z1nm}, k_{z2nm}, d)}{1 + G_h(k_{z1nm}, k_{z2nm}, d)R_h(k_{znm}, k_{z1nm})}\right] \cdot\left[\frac{1 - G_v(\epsilon_2 k_{z1i}, \epsilon k_{z2i}, d)}{1 + G_v(\epsilon_2 k_{z1i}, \epsilon k_{z2i}, d)R_v(\epsilon k_{zi}, k_{z1i})}\right] \quad (52)$$

$$g_\beta^{(1)} = \frac{-2ik_{zi}(k_0^2 - k_1^2)}{(\epsilon k_{znm} + k_{z1nm})(\epsilon k_{zi} + k_{z1i})} \cdot\left[\frac{1 + G_v(\epsilon_2 k_{z1i}, \epsilon k_{z2i}, d)}{1 + G_v(\epsilon_2 k_{z1i}, \epsilon k_{z2i}, d)R_v(\epsilon k_{zi}, k_{z1i})}\right] \cdot\left[\frac{1 + G_v(\epsilon_2 k_{z1nm}, \epsilon k_{z2nm}, d)}{1 + G_v(\epsilon_2 k_{z1nm}, \epsilon k_{z2nm}, d)R_v(\epsilon k_{znm}, k_{z1nm})}\right]$$

$$\cdot\left(\frac{\epsilon k_{\rho i}k_{\rho nm}}{k_0^2}-\frac{k_{z1i}k_{z1nm}}{k_0^2}c_{i,n}\cdot\left[\frac{1-G_v(\epsilon_2 k_{z1nm},\,\epsilon k_{z2nm},\,d)}{1+G_v(\epsilon_2 k_{z1nm},\,\epsilon k_{z2nm},\,d)}\right]\cdot\left[\frac{1-G_v(\epsilon_2 k_{z1i},\,\epsilon k_{z2i},\,d)}{1+G_v(\epsilon_2 k_{z1i},\,\epsilon k_{z2i},\,d)}\right]\right) \tag{53}$$

for a vertically polarized incident field. In the above equations, $c_{i,n}$ and $s_{i,n}$ represent the cosine and sine functions

$$c_{i,n}=\frac{k_{xi}k_{xn}+k_{yi}k_{ym}}{k_{\rho i}k_{\rho nm}} \tag{54}$$

$$s_{i,n}=\frac{k_{xi}k_{ym}-k_{yi}k_{xn}}{k_{\rho i}k_{\rho nm}} \tag{55}$$

while the terms in brackets are due to the presence of the layered medium. Note these terms become unity as the reflection at $z=-d$ vanishes (i.e., G_h and G_v approach zero), and first order results for a homogeneous medium are obtained. These results illustrate the "Bragg scatter" phenomenon of first order perturbation theory, since scattered fields at a particular angle [i.e., $(n,\,m)$] are directly proportional to the amplitude of a particular surface Fourier component. Equations (50)–(53) are identical to those in [12] when backscattering is considered but apply for general bistatic scattering angles.

A second order correction to the specularly reflected fields in region zero can also be derived as

$$\zeta_{0,0}^{(2)}=\sum_m\sum_n|h_{n,m}|^2 g_\zeta^{(2)}(k_{xi},\,k_{yi},\,k_{xn},\,k_{ym}) \tag{56}$$

where $\zeta=\alpha$ or β, and $g_\zeta^{(2)}$ is a corresponding function. For a horizontally polarized incident field, see (57) and (58), shown at the bottom of the page. For a vertically polarized incident field, see (59), shown at the bottom of the page, and $g_\alpha^{(2)}$ is -1 times $g_\beta^{(2)}$ for horizontal incidence in (58). The above results reduce to the second order specular reflection coefficient corrections described in [2] when the reflections at $z=-d$ vanish, except for a minus sign difference in cross polarized terms due to differing coordinate systems.

$$g_\alpha^{(2)}=\frac{-2k_{zi}(k_0^2-k_1^2)}{(k_{zi}+k_{z1i}Z_h(k_{z1i},\,k_{z2i},\,d))^2}\left\{k_{z1i}Z_h(k_{z1i},\,k_{z2i},\,d)+\frac{k_{znm}k_{z1nm}(1-\epsilon)Z_v(\epsilon_2 k_{z1nm},\,\epsilon k_{z2nm},\,d)}{\epsilon k_{znm}+k_{z1nm}Z_v(\epsilon_2 k_{z1nm},\,\epsilon k_{z2nm},\,d)}+c_{i,n}^2\cdot\left(\frac{k_0^2-k_1^2}{k_{znm}+k_{z1nm}Z_h(k_{z1nm},\,k_{z2nm},\,d)}-\frac{k_{znm}k_{z1nm}(1-\epsilon)Z_v(\epsilon_2 k_{z1nm},\,\epsilon k_{z2nm},\,d)}{\epsilon k_{znm}+k_{z1nm}Z_v(\epsilon_2 k_{z1nm},\,\epsilon k_{z2nm},\,d)}\right)\right\} \tag{57}$$

$$g_\beta^{(2)}=\frac{-2k_{zi}(k_0^2-k_1^2)}{(\epsilon k_{zi}+k_{z1i}Z_v(\epsilon_2 k_{z1i},\,\epsilon_1 k_{z2i},\,d))(k_{zi}+k_{z1i}Z_h(k_{z1i},\,k_{z2i},\,d))}\cdot\left\{-s_{i,n}c_{i,n}\frac{k_{z1i}(\epsilon-1)Z_v(\epsilon_2 k_{z1i},\,\epsilon_1 k_{z2i},\,d)}{k_{znm}+k_{z1nm}Z_h(k_{z1nm},\,k_{z2nm},\,d)}\cdot\left(-k_0+\frac{k_{znm}k_{z1nm}Z_v(\epsilon_2 k_{z1nm},\,\epsilon k_{z2nm},\,d)(k_{znm}+k_{z1nm}Z_h(k_{z1nm},\,k_{z2nm},\,d))}{k_0(\epsilon k_{znm}+k_{z1nm}Z_v(\epsilon_2 k_{z1nm},\,\epsilon k_{z2nm},\,d))}\right)-s_{i,n}\frac{\epsilon k_{\rho i}k_{\rho nm}(k_{znm}+k_{z1nm}Z_v(\epsilon_2 k_{z1nm},\,\epsilon k_{z2nm},\,d))}{k_0(\epsilon k_{znm}+k_{z1nm}Z_v(\epsilon_2 k_{z1nm},\,\epsilon k_{z2nm},\,d))}\right\}. \tag{58}$$

$$g_\beta^{(2)}=\frac{-2k_{zi}(k_0^2-k_1^2)}{(\epsilon k_{zi}+k_{z1i}Z_v(\epsilon_2 k_{z1i},\,\epsilon_1 k_{z2i},\,d))^2}\left\{\frac{-\epsilon k_{\rho i}^2k_{\rho nm}^2(\epsilon-1)}{k^2(\epsilon k_{znm}+k_{z1nm}Z_v(\epsilon_2 k_{z1nm},\,\epsilon k_{z2nm},\,d))}-\epsilon k_{z1i}Z_v(\epsilon_2 k_{z1i},\,\epsilon_1 k_{z2i},\,d)-\frac{k_{z1i}^2(Z_v(\epsilon_2 k_{z1i},\,\epsilon_1 k_{z2i},\,d))^2(1-\epsilon)}{k_{znm}+k_{z1nm}Z_h(k_{z1nm},\,k_{z2nm},\,d)}+c_{i,n}\left(\frac{2\epsilon k_{\rho i}k_{\rho nm}k_{z1i}Z_v(\epsilon_2 k_{z1i},\,\epsilon_1 k_{z2i},\,d)}{k^2}\right)\left(\frac{k_{znm}+k_{z1nm}Z_v(\epsilon_2 k_{z1nm},\,\epsilon k_{z2nm},\,d)}{\epsilon k_{znm}+k_{z1nm}Z_v(\epsilon_2 k_{z1nm},\,\epsilon k_{z2nm},\,d)}\right)+c_{i,n}^2\left(\frac{k_{z1i}^2(Z_v(\epsilon_2 k_{z1i},\,\epsilon_1 k_{z2i},\,d))^2(1-\epsilon)}{k_{znm}+k_{z1nm}Z_h(k_{z1nm},\,k_{z2nm},\,d)}-\frac{k_{z1i}^2k_{znm}k_{z1nm}(1-\epsilon)Z_v(\epsilon_2 k_{z1nm},\,\epsilon k_{z2nm},\,d)(Z_v(\epsilon_2 k_{z1i},\,\epsilon_1 k_{z2i},\,d))^2}{k^2(\epsilon k_{znm}+k_{z1nm}Z_v(\epsilon_2 k_{z1nm},\,\epsilon k_{z2nm},\,d))}\right)\right\}. \tag{59}$$

Polarimetric brightness temperatures of a periodic surface can be calculated through the application of Kirchhoff's Law

$$\overline{T}_B = \begin{bmatrix} T_{Bh} \\ T_{Bv} \\ T_U \\ T_V \end{bmatrix} = T_s \left(\begin{bmatrix} 1 - r_h \\ 1 - r_v \\ -r_U \\ -r_V \end{bmatrix} \right) \tag{60}$$

where T_{Bh} and T_{Bv} are the brightness temperatures measured by horizontally and vertically polarized antennas, respectively, T_U and T_V are proportional to the real and imaginary parts of the correlation between fields in horizontal and vertical polarizations, respectively ([2]), and T_s refers to the layered medium physical temperature in Kelvin (assumed constant throughout the layered medium). Total reflectivities for the periodic surface to second order in surface height are shown in (61), at the bottom of the next page, where the first term is the reflectivity of the layered medium with a flat interface, and the following two terms are the Bragg scattering and reflection coefficient correction contributions, respectively. In the aforementioned equations, the subscripts hh and hv refer to g_α functions with horizontal incidence and vertical incidence, respectively, while vh and vv refer to g_β functions with horizontal and vertical incidence, respectively. Note that both of the summations are in terms of sums over the periodic surface power spectral density $|h_{n,m}|^2$ and can be combined into a single term that expresses the correction to brightness temperatures caused by surface roughness. In the limit that surface periods become large compared to both the electromagnetic wavelength and any roughness features, the sums can be replaced with integrals over the continuous power spectral density $W(k_{xn} - k_{xi}, k_{ym} - k_{yi}) = (|h_{n,m}|^2/\delta k_x \delta k_y)$, where $\delta k_x = (2\pi/P_x)$ and $\delta k_y = (2\pi/P_y)$. The final result for continuous surface brightness temperatures is shown in (62), at the bottom of the page, where the new $\tilde{g}$ functions include both the Bragg scatter and reflection coefficient correction terms described previously and are functions of the radiometer polar observation angle θ_i, the radiometer azimuthal observation angle ϕ_i, the layered medium properties ϵ, ϵ_2, and d, and the integration variables k'_ρ and ϕ'. Note also that a coordinate shift has been made in the above integration: $\tilde{g}$ functions are evaluated as in (61), except that $k_{xn} = k_{xi} + k'_\rho \cos\phi'$ and $k_{ym} = k_{yi} + k'_\rho \sin\phi'$. The dependence of the $\tilde{g}$ functions on $\phi' - \phi_i$ is found from (61), and the dependence on ϵ_2 is replaced by a dependence on R_h and R_v at $z = -d$ in the case of a general layered medium. Equation (62) expresses the brightness temperature of a layered medium bounded by a slightly rough interface in terms of the brightness temperature of the layered medium with a flat interface and a roughness correction. The roughness correction is obtained through an integration of the surface power spectral density W weighted by the $\tilde{g}$ weighting functions, which are distinct for each polarimetric quantity. Studies of these weighting functions therefore allow the physics of rough surface thermal emission to be examined independent of the particular surface power spectral density and are considered in the next section.

IV. Study of Weighting Functions for Isotropic Surfaces

To simplify the analysis, assume that an isotropic surface is considered (i.e., one with no directional properties) so that U and V brightnesses are zero [2] and so that the roughness correction becomes

$$\begin{aligned} \Delta T_{B\gamma} &= -T_s \left(\int_0^\infty dk'_\rho k'_\rho W(k'_\rho) \int_0^{2\pi} d\phi' \right. \\ &\qquad \left. \tilde{g}_\gamma \cdot (f, \theta_i, \epsilon, \epsilon_2, d, k'_\rho, \phi' - \phi_i) \right) \\ &= -T_s \left(\int_0^\infty dk'_\rho k'_\rho W(k'_\rho) \tilde{g}_{\gamma,0}(f, \theta_i, \epsilon, \epsilon_2, d, k'_\rho) \right) \end{aligned} \tag{63}$$

$$\begin{aligned} \begin{bmatrix} r_h \\ r_v \\ r_U \\ r_V \end{bmatrix} &= \begin{bmatrix} |R_{Hl}|^2 \\ |R_{Vl}|^2 \\ 0 \\ 0 \end{bmatrix} + \sum_m \sum_n |h_{n,m}|^2 \frac{\mathrm{Re}\{k_{znm}\}}{k_{zi}} \begin{bmatrix} |g_{hh}^{(1)}(k_{znm})|^2 + |g_{vh}^{(1)}(k_{znm})|^2 \\ |g_{hv}^{(1)}(k_{znm})|^2 + |g_{vv}^{(1)}(k_{znm})|^2 \\ 2\mathrm{Re}\{g_{hv}^{(1)}(k_{znm}) g_{hh}^{(1)*}(k_{znm}) + g_{vv}^{(1)}(k_{znm}) g_{vh}^{(1)*}(k_{znm})\} \\ 2\mathrm{Im}\{g_{hv}^{(1)}(k_{znm}) g_{hh}^{(1)*}(k_{znm}) + g_{vv}^{(1)}(k_{znm}) g_{vh}^{(1)*}(k_{znm})\} \end{bmatrix} \\ &\quad + \sum_m \sum_n |h_{n,m}|^2 \begin{bmatrix} 2\mathrm{Re}\{R_{Hl}^* g_{hh}^{(2)}(k_{xi}, k_{yi}, k_{xn}, k_{ym})\} \\ 2\mathrm{Re}\{R_{Vl}^* g_{vv}^{(2)}(k_{xi}, k_{yi}, k_{xn}, k_{ym})\} \\ 2\mathrm{Re}\{(R_{Hl}^* - R_{Vl}^*) g_{hv}^{(2)}(k_{xi}, k_{yi}, k_{xn}, k_{ym})\} \\ 2\mathrm{Im}\{(R_{Hl}^* + R_{Vl}^*) g_{hv}^{(2)}(k_{xi}, k_{yi}, k_{xn}, k_{ym})\} \end{bmatrix} \end{aligned} \tag{61}$$

$$\begin{bmatrix} T_{Bh} \\ T_{Bv} \\ T_U \\ T_V \end{bmatrix} = T_s \left(\begin{bmatrix} 1 - |R_{Hl}|^2 \\ 1 - |R_{Vl}|^2 \\ 0 \\ 0 \end{bmatrix} - \int_0^\infty dk'_\rho k'_\rho \int_0^{2\pi} d\phi' W(k'_\rho, \phi') \begin{bmatrix} \tilde{g}_h(f, \theta_i, \epsilon, \epsilon_2, d, k'_\rho, \phi' - \phi_i) \\ \tilde{g}_v(f, \theta_i, \epsilon, \epsilon_2, d, k'_\rho, \phi' - \phi_i) \\ \tilde{g}_U(f, \theta_i, \epsilon, \epsilon_2, d, k'_\rho, \phi' - \phi_i) \\ \tilde{g}_V(f, \theta_i, \epsilon, \epsilon_2, d, k'_\rho, \phi' - \phi_i) \end{bmatrix} \right) \tag{62}$$

where $\gamma = h$ or v. Studies of the $\tilde{g}_{\gamma,0}$ functions reveal further simplification if a factor of k_0^2 is removed

$$\Delta T_{B\gamma} = -T_s k_0^2 \cdot \left(\int_0^\infty dk'_\rho k'_\rho W(k'_\rho) \tilde{\tilde{g}}_{\gamma,0}(\theta_i, \epsilon, \epsilon_2, k_0 d, k'_\rho/k_0) \right) \tag{64}$$

illustrating that the $\tilde{\tilde{g}}$ weighting functions do not explicitly depend on frequency if length scales relative to the electromagnetic wavelength (i.e., $k_0 d$ and k'_ρ/k_0) are considered.

Fig. 2(a) plots $\tilde{\tilde{g}}_{h,0}$ and $\tilde{\tilde{g}}_{v,0}$ versus k'_ρ/k_0 for a two layer medium with $d = 0.1\lambda$, $\epsilon = 7.5 + i0.67$, $\epsilon_2 = 3 + i\ 0.08$ (intended to model a clay medium at 3 GHz with upper and lower layer moisture contents of approximately 20 and 5%) and for $\theta_i = 30°$. Logarithmic scales are used for both the horizontal and vertical axes to enable a large range of scales to be observed. Signs of these functions (defined as $+1$ for positive values and -1 for negative values) are displayed in Fig. 2 plot (b), with the $\tilde{\tilde{g}}_{h,0}$ and $\tilde{\tilde{g}}_{v,0}$ sign curves shifted by $+2$ and -2, respectively, to enable them to be distinguished. Note the constant valued weighting functions obtained as k'_ρ/k_0 becomes small (large length scales in the spectrum relative to λ). Notating the value of this constant as $\tilde{\tilde{g}}_{\gamma,0}(\theta_i, \epsilon, \epsilon_2, k_0 d, 0)$, Fig. 2 plots (c) and (d) illustrate the scaled difference functions

$$\tilde{\tilde{g}}_{\gamma,s} = \frac{\tilde{\tilde{g}}_{\gamma,0}(\theta_i, \epsilon, \epsilon_2, k_0 d, k'_\rho/k_0) - \tilde{\tilde{g}}_{\gamma,0}(\theta_i, \epsilon, \epsilon_2, k_0 d, 0)}{(k'_\rho/k_0)^2} \tag{65}$$

and their signs, respectively. Roughness induced changes in brightnesses can then be rewritten as

$$\begin{aligned}\Delta T_{B\gamma} &= -T_s k_0^2 \left(\tilde{\tilde{g}}_{\gamma,0}(\theta_i, \epsilon, \epsilon_2, k_0 d, 0) \int_0^\infty dk'_\rho k'_\rho W(k'_\rho) + \frac{1}{k_0^2} \int_0^\infty dk'_\rho k'^3_\rho W(k'_\rho) \tilde{\tilde{g}}_{\gamma,s}(\theta_i, \epsilon, \epsilon_2, k_0 d, k'_\rho/k_0) \right) \\ &= -T_s \left(\frac{k_0^2 h^2}{2\pi} \tilde{\tilde{g}}_{\gamma,0}(\theta_i, \epsilon, \epsilon_2, k_0 d, 0) + \int_0^\infty dk'_\rho k'^3_\rho W(k'_\rho) \tilde{\tilde{g}}_{\gamma,s}(\theta_i, \epsilon, \epsilon_2, k_0 d, k'_\rho/k_0) \right) \end{aligned} \tag{66}$$

where h^2 is the surface height variance. The above equation shows that $\tilde{\tilde{g}}_{\gamma,0}(\theta_i, \epsilon, \epsilon_2, k_0 d, 0)$ indicates a dependence on the surface variance, while $\tilde{\tilde{g}}_{\gamma,s}(\theta_i, \epsilon, \epsilon_2, k_0 d, k'_\rho/k_0)$ represents a function that weights the spectrum in computing the surface slope variance.

Fig. 2 (a) and (c) both show the "critical phenomena" effects [17] observed in the homogeneous medium case, and the vertical lines included in plot (c) mark the boundaries of the region within which critical phenomena can occur. As in the homogeneous medium case, Fig. 2 (c) demonstrates that length scales both much larger than or comparable to the electromagnetic wavelength can contribute to the roughness-induced correction through $\tilde{\tilde{g}}_{\gamma,s}$. The importance of $\tilde{\tilde{g}}_{\gamma,s}$ contributions, however, depends strongly on the magnitude of the $(k_0^2 h^2/2\pi)\tilde{\tilde{g}}_{\gamma,0}(\theta_i, \epsilon, \epsilon_2, k_0 d, 0)$ product.

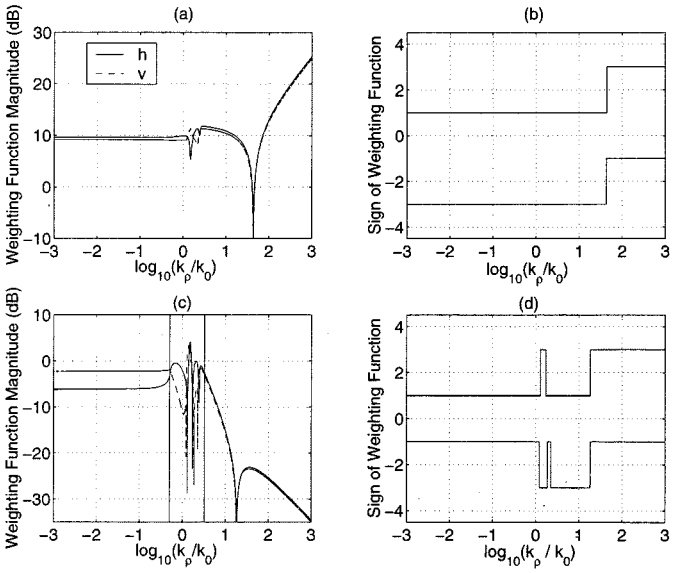

Fig. 2. Weighting functions for a two layer medium with $\theta_i = 30°$, $d = 0.1\lambda$, $\epsilon = 7.5 + i\ 0.67$ and $\epsilon_2 = 3 + i\ 0.08$. (a) Magnitude of weighting functions $\bar{g}_{\gamma,0}$. (b) Sign of weighting functions $\bar{g}_{\gamma,0}$. (c) Magnitude of weighting functions $\bar{g}_{\gamma,s}$. (d) Magnitude of weighting functions $\bar{g}_{\gamma,s}$. Note the sign curves are shifted by $+2$ and -2 for h and v polarizations, respectively.

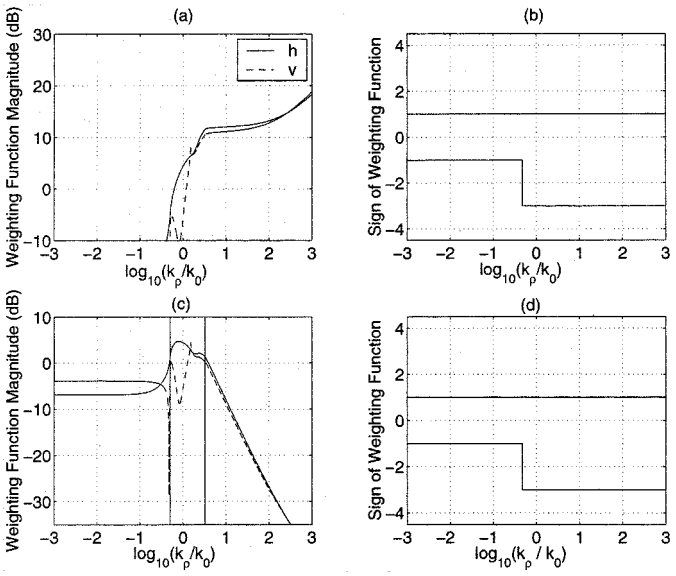

Fig. 3. Same as Fig. 2, but for $\epsilon_2 = 7.5 + i\ 0.67$.

To clarify the relationship between emission for a rough surface bounding, a two layer medium versus a homogeneous medium, Fig. 3 (a)–(d) illustrate the same functions as in Fig. 2, except that ϵ_2 is modified to equal ϵ, so that a homogeneous medium exists below the rough surface. Note the dramatic change in plot (a), as the constant-valued weighting functions for small k'_ρ/k_0 no longer occur since $\tilde{\tilde{g}}_{\gamma,0}(\theta_i, \epsilon, \epsilon, k_0 d, 0) = 0$. Thus, with a homogeneous medium, a surface height variance-dependent term is not obtained, resulting in a small slope approximation [7]. As is evident from Fig. 2 (a) however, height-dependent terms do not vanish in the layered medium case, and the theory remains a small height expansion.

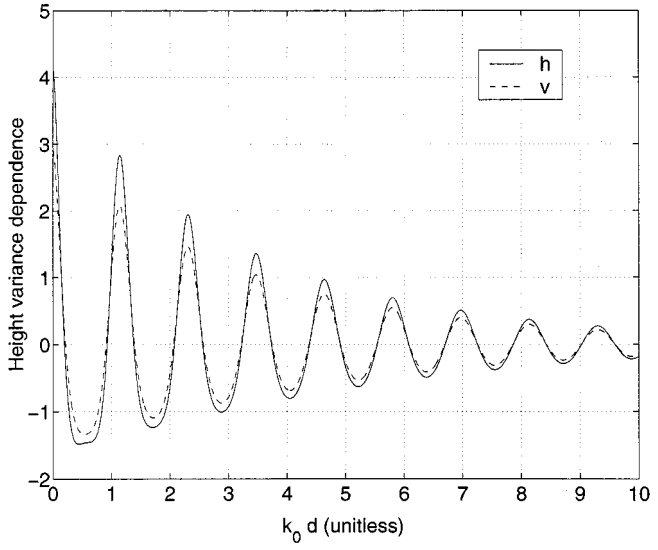

Fig. 4. Surface height dependent term $(1/2\pi)\bar{\tilde{g}}_{\gamma,0}(\theta_i,\ \epsilon,\ \epsilon_2,\ k_0 d,\ 0)$ for the layered medium of Fig. 2 versus $k_0 d$.

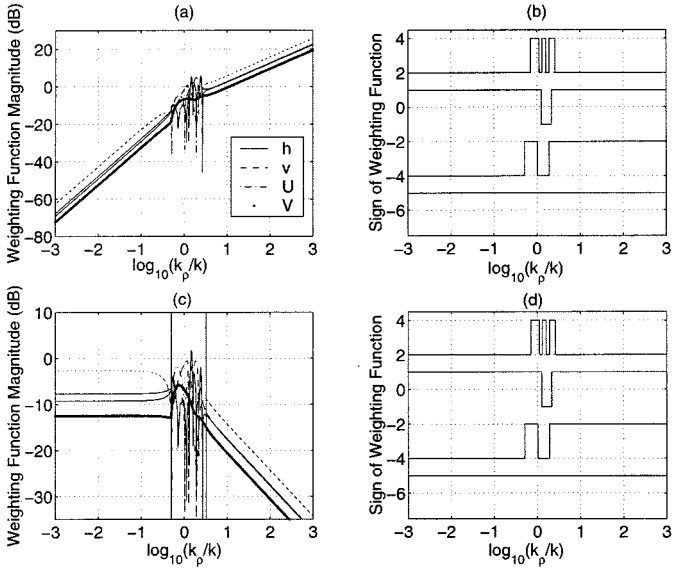

Fig. 5. Second harmonic weighting functions for a two layer medium with $\theta_i = 30°$, $d = 0.1\lambda$, $\epsilon = 7.5 + i\ 0.67$, and $\epsilon_2 = 3 + i\ 0.08$. (a) Magnitude of weighting functions $\bar{g}_{\gamma,2}$. (b) Sign of weighting functions $\bar{g}_{\gamma,2}$. (c) Magnitude of weighting functions $\bar{g}_{\gamma,2}/(k'_\rho/k_0)^2$. (d) Magnitude of weighting functions $\bar{g}_{\gamma,2}/(k'_\rho/k_0)^2$. Note the sign curves are shifted by $+3$, 0, -3, and -6 for h, v, U, and V polarizations, respectively.

Note also that the magnitude of the height variance-dependent correction is determined by $\tilde{\tilde{g}}_{\gamma,0}(\theta_i,\ \epsilon,\ \epsilon_2,\ k_0 d,\ 0)$, which remains a function of the layered medium properties. Thus, convergence of the series is not determined by rough surface parameters alone. An estimate of the accuracy of the second order correction for surfaces with small slopes can be obtained by examining the magnitude of the $(k_0^2 h^2/2\pi)\tilde{\tilde{g}}_{\gamma,0}(\theta_i,\ \epsilon,\ \epsilon_2,\ k_0 d,\ 0)$ product. Small values of this product ($\leq$0.025) should indicate that the second order theory provides reasonable answers, while larger values may require a higher order theory in order to obtain accurate predictions. Fig. 4 plots $(1/2\pi)\tilde{\tilde{g}}_{\gamma,0}(\theta_i,\ \epsilon,\ \epsilon_2,\ k_0 d,\ 0)$ for the two layer medium above as a function of $k_0 d$. Note the periodic increases that occur. A reasonable prediction of roughness-induced corrections can still be obtained for depths at which $(1/2\pi)\tilde{\tilde{g}}_{\gamma,0}(\theta_i,\ \epsilon,\ \epsilon_2,\ k_0 d,\ 0)$ becomes large, but a correspondingly smaller surface height variance would be required. A verification of the suggested convergence test was performed through comparison with a numerical solution of the SPM equations as described in [18], which enabled the fourth order correction to be determined. Choosing $|(1/2\pi)k_0^2 h^2 \tilde{\tilde{g}}_{\gamma,0}(\theta_i,\ \epsilon,\ \epsilon_2,\ k_0 d,\ 0)| \leq 0.025$ [or equivalently, $kh \leq (0.4/\sqrt{|\tilde{\tilde{g}}_{\gamma,0}(\theta_i,\ \epsilon,\ \epsilon_2,\ k_0 d,\ 0)|})$] was found in several tests to provide fourth order corrections significantly smaller than second order, although cases in which $\tilde{\tilde{g}}_{\gamma,0}(\theta_i,\ \epsilon,\ \epsilon_2,\ k_0 d,\ 0)$ vanishes remain problematic and require careful consideration. Tests of the higher order theory indicate that a small slope expansion is not necessarily achieved when $\tilde{\tilde{g}}_{\gamma,0}(\theta_i,\ \epsilon,\ \epsilon_2,\ k_0 d,\ 0)$ vanishes unless the physical configuration approaches that of the homogeneous medium (i.e., region one becomes sufficiently lossy to obscure reflections from region two.)

V. Study of Weighting Functions for Asymmetric Surfaces

For surfaces that are not symmetric in azimuth, brightness temperatures become a function of the radiometer azimuthal observation angle ϕ_i and U, and V polarimetric brightnesses become nonzero. In this case, the roughness-induced correction is

$$\Delta T_{B\gamma} = -T_s \left(\int_0^\infty dk'_\rho k'_\rho \int_0^{2\pi} d\phi' W(k'_\rho,\ \phi') \tilde{g}_\gamma(f,\ \theta_i,\ \epsilon,\ \epsilon_2,\ d,\ k'_\rho,\ \phi' - \phi_i) \right) \tag{67}$$

where $\gamma = h,\ v,\ U$, or V. The above expression can be simplified as described in [17] through an expansion of both $W(k'_\rho,\ \phi')$ and $\tilde{g}_\gamma$ into Fourier series in azimuth. It is also assumed that the surface spectrum contains only even cosine harmonics. The resulting expression for the roughness-induced correction is shown in (68), at the bottom of the page, where

$$\Delta T_{B\gamma} = -T_s k_0^2 \left(\begin{bmatrix} \int_0^\infty dk'_\rho k'_\rho \tilde{\tilde{g}}_{\gamma,0}(k'_\rho/k_0) W_0(k'_\rho) \\ 0 \end{bmatrix} + \sum_{n=1}^{\infty} \begin{bmatrix} 2\cos(n\phi_i) \int_0^\infty dk'_\rho k'_\rho \operatorname{Re}\{\tilde{\tilde{g}}_{\gamma,n}(k'_\rho/k_0)\} W_n(k'_\rho) \\ -2\sin(n\phi_i) \int_0^\infty dk'_\rho k'_\rho \operatorname{Im}\{\tilde{\tilde{g}}_{\gamma,n}(k'_\rho/k_0)\} W_n(k'_\rho) \end{bmatrix} \right) \tag{68}$$

the upper row applies for h and v brightnesses, while the lower row applies for U and V. In the above equation

$$\tilde{\tilde{g}}_{\gamma,n}(k'_\rho/k_0) = \frac{1}{k_0^2}\int_0^{2\pi} d\phi' e^{in\phi'}\tilde{g}_\gamma(f,\theta_i,\epsilon,\epsilon_2,d,k'_\rho,\phi') \tag{69}$$

and is also a function of θ_i, ϵ, ϵ_2, and $k_0 d$, while

$$W_n(k'_\rho) = \frac{1}{2\pi}\int_0^{2\pi} d\phi' e^{-in\phi'} W(k'_\rho,\phi'). \tag{70}$$

Equation (68) demonstrates that particular azimuthal harmonics of polarimetric brightness temperatures [i.e., the $\cos(n\phi_i)$ and $\sin(n\phi_i)$ terms] are given by integrals of a distinct weighting function for each azimuthal harmonic ($\tilde{\tilde{g}}_{\gamma,n}(k'_\rho/k_0)$), multiplied with the corresponding surface spectrum harmonic $W_n(k'_\rho)$. Under these definitions, the zeroth harmonic weighting functions are identical to those considered in Figs. 2 and 3.

Fig. 5 plots the second harmonic weighting functions $\mathrm{Re}\{\tilde{\tilde{g}}_{\gamma,2}\}$ for h and v and $\mathrm{Im}\{\tilde{\tilde{g}}_{\gamma,2}\}$ for U and V versus k'_ρ/k_0 for the case considered in Fig. 2. Plot (a) in this figure illustrates the magnitudes of the second harmonic weighting functions in dB, while plot (b) illustrates their signs. Note again the four sign functions are shifted in steps of 3 to allow the curves to be more easily distinguished. The constant-valued weighting functions for small k'_ρ/k_0 observed in Fig. 2 are not obtained in this case, indicating that the second order SPM produces a surface slope-dependent term for second azimuthal harmonics. Plots (c) and (d) of Fig. 5 illustrate the weighting functions divided by $(k'_\rho/k_0)^2$, as in plots (c) and (d) of Fig. 2 and confirm the slope dependence. A slope rather than height dependence for azimuthal harmonics with $n > 0$ would be advantageous, particularly in studies of sea surface emission. However, further tests with the numerical SPM solution (again, implemented following the procedure in [18]) showed that azimuthal harmonics with $n > 0$ depend directly on the surface height variance at fourth and higher orders. Thus, the theory remains an expansion in surface height for all azimuthal harmonics of surface brightness temperatures, even though the second order prediction of azimuthal harmonics with $n > 0$ does not directly involve the surface height variance. Predictions of the second order theory for second harmonic coefficients were found adequate in cases for which the convergence requirement specified in Section IV was satisfied.

VI. Sample Results

To illustrate the influence of layered media on roughness-induced emission corrections, sample brightness temperatures are considered in this section. Fig. 6 illustrates results for surfaces with $T_s = 283$ K and with an isotropic, Gaussian roughness spectrum, completely characterized by the root mean squared (rms) surface height h and correlation length l parameters. Note a Gaussian roughness spectrum is not necessarily realistic for soil surfaces, but is commonly applied in theoretical studies due to its simplicity. Roughness induced brightness temperature corrections for the two layer medium considered in Fig. 2

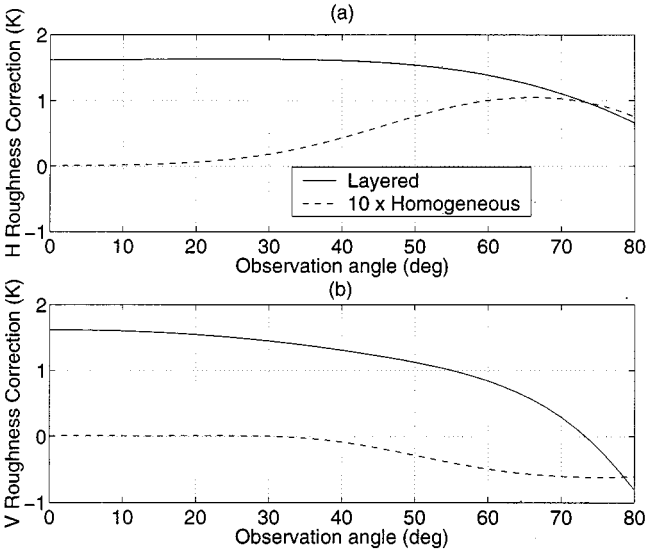

Fig. 6. Comparison of roughness induced brightness corrections for a two layer medium with $d = 0.1\lambda$, $\epsilon = 7.5 + i\ 0.67$, and $\epsilon_2 = 3 + i\ 0.08$ with a homogeneous medium $\epsilon_2 = 7.5 + i\ 0.67$ versus radiometer polar observation angle. The surface has an isotropic Gaussian roughness spectrum with $h = 0.01\lambda$ and $l = \lambda$. (a) Horizontal polarization and (b) vertical polarization. Note that homogeneous medium results are multiplied by ten in these plots.

and for $h = 0.01\lambda$, $l = \lambda$ are plotted versus observation angle in Fig. 6 and compared with those for a homogeneous medium with $\epsilon_2 = \epsilon$. Note the significant differences observed, both in the amplitude of roughness corrections and in their variations with observation angle. Homogeneous medium roughness corrections plotted in Fig. 6 are multiplied by ten to make their variations more clear. Height-dependent factors for all the cases shown were found to be <0.006, so that the second order correction should be accurate. Clearly, the presence of a layered medium below a rough interface can cause large changes in the influence of surface roughness on the medium boundary. Brightness temperatures for the flat surface medium are of course significantly different in the homogeneous and layered medium cases as well.

Fig. 7 illustrates the dependence of roughness induced emission corrections on layer depth d. The configuration is the same as that of Fig. 6 and for polar observation angle 30°. Note the oscillatory pattern observed versus depth, indicating the presence of coherent effects that are not disrupted by the small roughness used. Homogeneous medium roughness corrections for this case are less than 0.02 K in both polarizations.

Fig. 8 plots second harmonic coefficients of brightness temperatures versus observation angle for surfaces with an anisotropic Gaussian roughness spectrum with $h = 0.02\lambda$, $l_x = 0.5\lambda$, and $l_y = 1\lambda$, where l_x and l_y represent the correlation lengths in the x and y directions, respectively. Parameters of the layered medium are the same as those of previous examples, and again layered medium results are compared with those of a homogeneous medium. In this rougher surface case, height dependent factors remain <0.025 for all cases illustrated, so that second order theory predictions should be reasonable. Again the results show that the presence of a layered medium can cause significant changes in azimuthal variations of brightness temperatures, although the differences are smaller than those

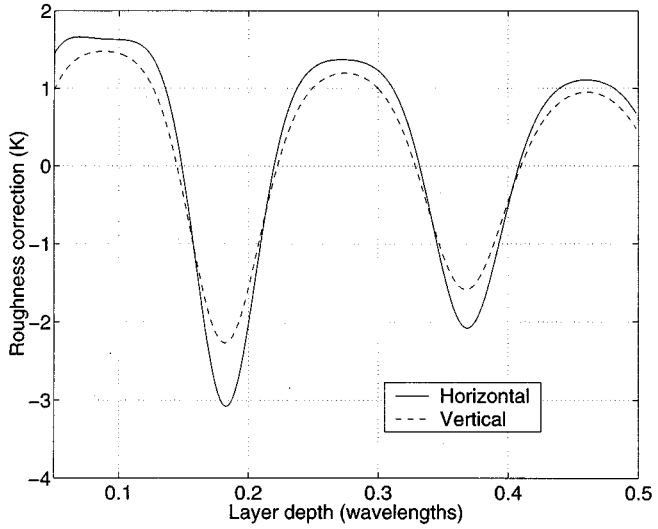

Fig. 7. Layer depth dependence of roughness induced brightness corrections for a two layer medium with $\epsilon = 7.5 + i\ 0.67$ and $\epsilon_2 = 3 + i\ 0.08$ at 30° polar observation angle. The surface has an isotropic Gaussian roughness spectrum with $h = 0.01\lambda$ and $l = \lambda$.

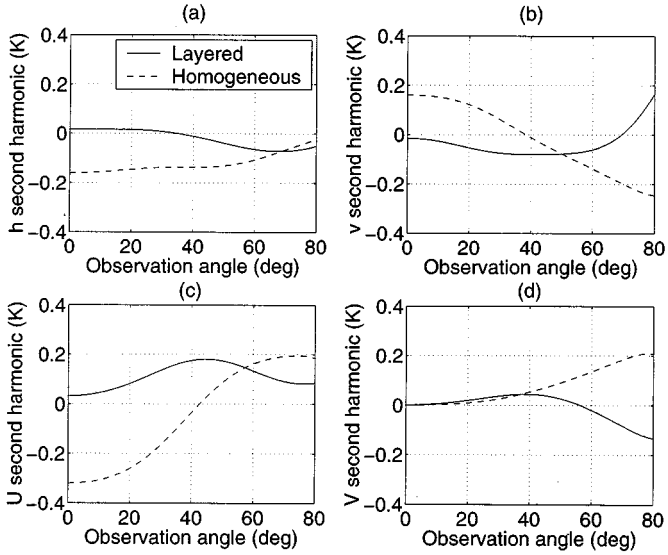

Fig. 8. Comparison of second harmonic brightness temperatures for a two layer medium with $d = 0.1\lambda$, $\epsilon = 7.5 + i\ 0.67$, and $\epsilon_2 = 3 + i\ 0.08$ with a homogeneous medium $\epsilon_2 = 7.5 + i\ 0.67$ versus radiometer polar observation angle. The surface has a Gaussian roughness spectrum with $h = 0.2\lambda$, $l_x = 0.5\lambda$, and $l_y = \lambda$. (a) Horizontal polarization, (b) vertical polarization, (c) U brightness, and (d) V brightness.

of Fig. 6 due to the absence of a height variance dependence in the second order prediction of second harmonic coefficients.

VII. Conclusions

Expressions for slightly rough surface-induced corrections to layered medium thermal emission have been derived through the small perturbation method in this paper. Results show that an expansion in surface height, as opposed to surface slope, is obtained, but accurate predictions can still be computed from the theory as long as the specified convergence rules are followed. The theory can be applied to problems in the remote sensing of soil moisture, sea ice, or sea surfaces to assess the effect of surface roughness on layered medium brightness temperatures. Typically, surface roughness corrections are expected to be small in microwave passive remote sensing, but current sensors are sufficiently accurate to observe these variations in many cases. Understanding and including rough surface effects in retrieval models can therefore potentially lead to more accurate sensing of layered medium parameters. The modification proposed in [12] for modeling scattering from a finite size object buried beneath an interface can also be applied in the emission equations to produce an approximate emission theory for a finite object buried beneath the ground. Studies of microwave radiometry for buried object detection like those of [10], [11], but including rough interface effects can therefore also be performed with the theory developed.

Finally, note that the change from a small slope to small height theory in the layered medium case raises some interesting issues, in particular regarding the magnitude of a change in permittivity in the medium required to introduce a significant height dependence. This question can be important in studies of sea surface remote sensing, since the height variance of sea surfaces is typically very large with respect to the wavelength at higher microwave frequencies, making a small height theory of sea surface emission impractical. The convergence expressions proposed can be applied to address these questions for a specified layered medium, but a more accurate emission theory will be needed in cases for which the convergence requirements are not satisfied.

References

[1] L. Tsang and R. W. Newton, "Microwave emissions from soils with rough surfaces," *J. Geophys. Res.*, vol. 87, pp. 9017–9024, 1982.

[2] S. H. Yueh, R. Kwok, F. K. Li, S. V. Nghiem, and W. J. Wilson, "Polarimetric passive remote sensing of ocean wind vectors," *Radio Sci.*, vol. 29, pp. 799–814, 1994.

[3] S. H. Yueh, "Modeling of wind direction signals in polarimetric sea surface brightness temperatures," *IEEE Trans. Geosci. Remote Sensing*, vol. 35, pp. 1400–1418, 1997.

[4] D. B. Kunkee and A. J. Gasiewski, "Simulation of passive microwave wind direction signatures over the ocean using an asymmetric-wave geometrical optics model," *Radio Sci.*, vol. 32, p. 59, 1997.

[5] V. G. Irisov, "Microwave radiation from a weakly non-Gaussian surface," in *Int. Geoscience and Remote Sensing Symp. '98 Conf. Proc.*, vol. 5, 1998, pp. 2329–2332.

[6] A. K. Fung and M. F. Chen, "Emission from an inhomogeneous layer with irregular surfaces," *Radio Sci.*, vol. 16, pp. 289–298, 1981.

[7] V. G. Irisov, "Small-slope expansion for thermal and reflected radiation from a rough surface," *Waves Random Media*, vol. 7, pp. 1–10, 1997.

[8] A. G. Voronovich, *Wave Scattering from Rough Surfaces*. Berlin, Germany: Springer-Verlag, 1994.

[9] M. Zhang and J. T. Johnson, "Theoretical studies of ocean polarimetric brightness signatures," in *Int. Geoscience and Remote Sensing Symp. '98 Conf. Proc.*, vol. 5, Seattle, WA, 1998, pp. 2333–2335.

[10] G. De Amici, B. Hauss, and L. Yujiri, "Detection of landmines via a passive microwave radiometer," in *Proc. SPIE*, vol. 3710, 1999.

[11] J. T. Johnson, "Theoretical study of microwave radiometry for buried object detection," in *Proc. SPIE*, vol. 4098, 2000.

[12] I. M. Fuks, "Radar contrast polarization dependence on subsurface sensing," in *Int. Geoscience and Remote Sensing Symp. '98 Conf. Proc.*, vol. 3, 1998, pp. 1455–1459.

[13] I. M. Fuks and A. G. Voronovich, "Wave diffraction by rough interfaces in an arbitrary plane layered medium," *Waves Random Media*, vol. 10, pp. 253–272, 2000.

[14] P. I. Arseev, "Perturbation theory for the Green's function of an electromagnetic field on a rough surface," *Sov. Phys. JETP*, vol. 65, pp. 262–267, 1987.

[15] G. V. Rozhnov, "Electromagnetic wave diffraction by multilayer media with rough interfaces," *Sov. Phys. JETP*, vol. 69, pp. 646–651, 1989.

[16] N. P. Zhuk, A. V. Frankov, and A. G. Yarovoy, "Backward scattering of electromagnetic waves by the rough surface of a medium whose dielectric permittivity has an exponential profile," *Sov. J. Commun. Technol. Electron.*, vol. 38, pp. 108–111, 1993.

[17] J. T. Johnson and M. Zhang, "Theoretical study of the small slope approximation for ocean polarimetric thermal emission," *IEEE Trans. Geosci. Remote Sensing*, vol. 37, pp. 2305–2736, Sept. 1999.

[18] J. T. Johnson, "Third order small perturbation method for scattering from dielectric rough surfaces," *J. Opt. Soc. Amer. A*, vol. 16, no. 11, pp. 2720–2736, 1999.

[19] S. O. Rice, "Reflection of electromagnetic waves from slightly rough surfaces," *Commun. Pure Appl. Math*, vol. 4, pp. 361–378, 1951.

[20] G. R. Valenzuela, "Depolarization of EM waves by slightly rough surfaces," *IEEE Trans. Antennas Propagat.*, vol. AP-15, pp. 552–557, 1967.

Joel T. Johnson (M'96) received the B.E.E. degree from the Georgia Institute of Technology, Atlanta, in 1991, and the S.M. and Ph.D. degrees from the Massachusetts Institute of Technology, Cambridge, in 1993 and 1996, respectively.

He is currently an Associate Professor in the Department of Electrical Engineering and ElectroScience Laboratory, The Ohio State University, Columbus. His research interests are in the areas of microwave remote sensing, propagation, and electromagnetic wave theory.

Dr. Johnson is an Associate Member of commissions B and F of the International Union of Radio Science (URSI) and a member of Tau Beta Pi, Eta Kappa Nu, and Phi Kappa Phi. He received the 1993 best paper award from the IEEE Geoscience and Remote Sensing Society, and was named an Office of Naval Research Young Investigator, National Science Foundation Career awardee, and PECASE award recipient in 1997.